

Diffusion Model for Generative Image Denoising

Yutong Xie
Peking University

Mingze Yuan
Peking University

Bin Dong
Peking University

Quanzheng Li
Massachusetts General Hospital and Harvard Medical School

Abstract

In supervised learning for image denoising, usually the paired clean images and noisy images are collected or synthesised to train a denoising model. L2 norm loss or other distance functions are used as the objective function for training. It often leads to an over-smooth result with less image details. In this paper, we regard the denoising task as a problem of estimating the posterior distribution of clean images conditioned on noisy images. We apply the idea of diffusion model to realize generative image denoising. According to the noise model in denoising tasks, we redefine the diffusion process such that it is different from the original one. Hence, the sampling of the posterior distribution is a reverse process of dozens of steps from the noisy image. We consider three types of noise model, Gaussian, Gamma and Poisson noise. With the guarantee of theory, we derive a unified strategy for model training. Our method is verified through experiments on three types of noise models and achieves excellent performance.

1. Introduction

Image denoising [4, 16, 26] has been studied for many years. Suppose \mathbf{x} is a clean image and \mathbf{y} is a noisy image. The noise model can be written as follows:

$$\mathbf{y} = \mathbf{N}(\mathbf{x}; \mathbf{z}, \text{params}), \quad (1)$$

where \mathbf{z} represents the source of noise, params represents the parameters of the noise model. Current supervised learning methods focus on training a denoising model using paired clean images and noisy images. Hence, collecting or synthesising such pairs as training data is important. Usually, the denoising model is trained by the following loss function:

$$L(\theta) = \mathbb{E}_{\mathbf{x}, \mathbf{y}} [\mathbf{d}(\mathbf{x}, f(\mathbf{y}; \theta))], \quad (2)$$

where $f(\cdot; \theta)$ is a neural network and $\mathbf{d}(\cdot, \cdot)$ is a distance metric. This methodology of supervised learning in essence

is to define the denoising task as a training problem of determined mapping, from the noisy image \mathbf{y} to the clean one \mathbf{x} . However, the denoising model trained in this manner often leads to a result with average effect. From the Bayesian perspective, \mathbf{y} conditioned on \mathbf{x} follows a posterior distribution:

$$q(\mathbf{x} | \mathbf{y}) = \frac{q(\mathbf{y} | \mathbf{x}) q(\mathbf{x})}{q(\mathbf{y})}. \quad (3)$$

When $\mathbf{d}(\cdot, \cdot)$ in Eq. (2) is L2 norm distance, the trained model will be an estimation of $\mathbb{E}[\mathbf{x} | \mathbf{y}]$, i.e. the posterior mean. This explains why denoised result in usual supervised learning is over-smooth.

To avoid the average effect, we regard image denoising as a problem of estimation of posterior distribution $q(\mathbf{x} | \mathbf{y})$. Hence, we do not train a denoising model representing a determined mapping. Instead, we train a generative denoising model. Recently, the diffusion model has achieved tremendous success in the domain of image generative tasks [7, 10, 14, 18–20]. In the original diffusion model, diffusion process transform clean images \mathbf{x} to total Gaussian noise by adding little Gaussian noise and reducing the signal of \mathbf{x} step by step. The sampling of target distribution is realized by a reverse process with hundreds and thousands of iterations from total Gaussian noise to clean images. Though it is a powerful generative model, applying the diffusion model directly to image denoising is not a desirable way. Its illustration is shown in Fig. 1. It is time-consuming without any acceleration trick and does not fully utilize the residual information in noisy images. Interestingly, we observe that the diffusion process is similar to the noise model defined in Eq. (1), though the noise in diffusion model is limited to Gaussian noise and the signal of \mathbf{x} is reduced along the diffusion process. If the diffusion process is completely consistent with the noise model, it is possible that we can begin the reverse process with noisy images, rather than total Gaussian noise and reduce the iteration greatly. For this purpose, we propose a new diffusion model for denoising tasks. The diffusion process in our method is designed according to the specific noise model such that they are consistent. As a result, the reverse process

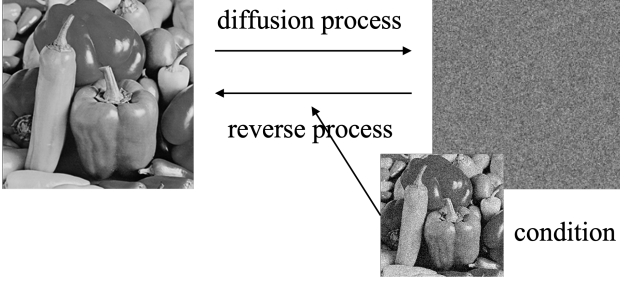


Figure 1. The illustration of applying the original diffusion model to image denoising.

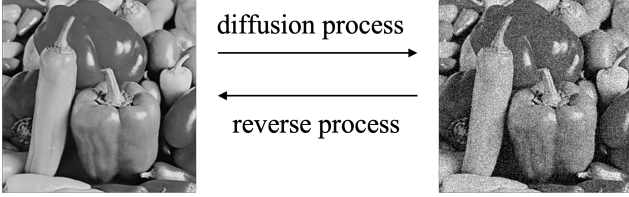


Figure 2. The illustration of proposed diffusion model for generative image denoising.

cess can start from the noisy image to realize sampling of $q(\mathbf{x} | \mathbf{y})$. We show the idea in Fig. 2. The details of design for diffusion process and reverse process, model training and sampling algorithms are described in Sec. 3.

In summary, our main contributions are: (1) We propose a new diffusion model designed for image denoising tasks. (2) We design the diffusion process, model training strategy and sampling algorithms for three types noise models, Gaussian, Gamma and Poisson. (3) Our experiments show that our proposed method is feasible.

2. Related Works

2.1. Supervised Learning

Learning from paired noisy-clean data is the mainstream in image denoising. Given paired noisy-clean data, it is straightforward to train supervised denoising methods. Albeit breakthrough performance has been achieved, the success of most existing deep denoisers heavily depend on supervised learning with large amount of paired noisy-clean images, which can be further divided into synthetic pairs [6, 9, 11, 23, 24, 26, 27, 29] and realistic pairs [1, 3, 8, 12, 17, 25, 28].

2.2. Original Diffusion Model

In the original diffusion model [7], the diffusion process is defined as:

$$\mathbf{x}_{t+1} = \alpha_t \mathbf{x}_t + \beta_t \mathbf{z}, t = 0, \dots, \quad (4)$$

where \mathbf{x}_0 is the clean image and \mathbf{z} follows the standard multi-variable Gaussian distribution. α_t is smaller than but near 1, and β_t is a very small value. When T is large enough, \mathbf{x}_T approximately follows the standard multi-variable Gaussian distribution. The reverse process is the inverse of the diffusion process. Therefore, the reverse process from a random Gaussian noise will lead to a sample of $q(\mathbf{x}_0)$.

3. Method

In this section, we provide a more detailed description of the presented approach. The organization is as follows: In Sec. 3.1 we introduce the basic framework of diffusion model designed for image denoising tasks. We present the application for three kinds of noise models in Sec. 3.2. Finally, Sec. 3.3 is the further discussion. All full proofs and derivation in this section can be found in Appendix.

3.1. Basic Framework

Suppose the noise model is known and we present it using following form:

$$\mathbf{y} = \mathbf{N}(\mathbf{x}; \mathbf{z}, \text{params}), \quad (5)$$

where \mathbf{z} represents the source of noise, params represents the parameters of the noise model. Here, $\mathbf{y} \sim \mathbf{y}$ is the noisy image and $\mathbf{x} \sim \mathbf{x}$ is the clean image. In this paper, we use different font to distinguish random variables and their samples like \mathbf{x} and \mathbf{x} . Our target is to realize sampling of $q(\mathbf{x} | \mathbf{y})$.

Since we adapt the idea of the original diffusion model, next we introduce the definition of diffusion process and reverse process.

3.1.1 Diffusion Process

Let $t = 0, 1, \dots, N$, we construct $N + 1$ random variables, \mathbf{x}_t , through a sequence of parameters in Eq. (5), $\{\text{params}_1, \text{params}_2, \dots, \text{params}_N\}$. Here, we define that $\mathbf{x}_0 = \mathbf{x}$, and let params_N be params in Eq. (5). Given $\mathbf{x}_0 \sim \mathbf{x}_0$, we have the following definition for diffusion process along t :

$$\mathbf{x}_t | \mathbf{x}_0 = \mathbf{N}(\mathbf{x}_0; \mathbf{z}, \text{params}_t), t = 1, \dots, N. \quad (6)$$

Such definition indicates that $\mathbf{x}_N = \mathbf{y}$. In the rest of this paper, for the sake of convenience we use \mathbf{x}_0 and \mathbf{x}_N to represent \mathbf{x} and \mathbf{y} respectively. Thus, \mathbf{x}_0 is a clean image and \mathbf{x}_N is the noisy image to be denoised. Usually, the sequence of $\{\text{params}_t\}$ can be regarded as a discrete sampling of a continuous (and monotonous) function $\text{Params}(t)$.

According to Eq. (6), $\mathbf{x}_t, t = 1, \dots, N - 1$ are also noisy images with a noise level different from \mathbf{x}_N . When $\text{params}_t, t = 1, \dots, N$, is fixed, the distribution of \mathbf{x}_t has

been determined by the distribution of \mathbf{x}_0 and the noise model. We have

$$q(\mathbf{x}_t) = \int_{\mathbf{x}_0} q(\mathbf{x}_t | \mathbf{x}_0) q(\mathbf{x}_0) d\mathbf{x}_0, \quad (7)$$

where $q(\mathbf{x}_0)$ is the probability density function of \mathbf{x}_0 and $q(\mathbf{x}_t | \mathbf{x}_0)$ is related to the noise model defined in Eq. (6). However, the relation between $\mathbf{x}_t, i = 1, \dots, N$ is not defined. Here, we do not provide the specific assumption for the relation and we discuss it in Sec. 3.2. Nevertheless, the diffusion process is related to the noise model in denoising task by the definition above.

3.1.2 Reverse Process

Since our target distribution is $q(\mathbf{x}_0 | \mathbf{x}_N)$ where \mathbf{x}_N is the given noisy image. Suppose the model is represented by $p_\theta(\mathbf{x}_0 | \mathbf{x}_N)$. We define the reverse process as a Markov chain:

$$p_\theta(\mathbf{x}_t | \mathbf{x}_{t+1}, \dots, \mathbf{x}_N) = p_\theta(\mathbf{x}_t | \mathbf{x}_{t+1}, \mathbf{x}_N). \quad (8)$$

Then, we have the following derivation:

$$\begin{aligned} p_\theta(\mathbf{x}_0 | \mathbf{x}_N) &= \int_{\mathbf{x}_{1:N-1}} p_\theta(\mathbf{x}_0, \mathbf{x}_1, \dots, \mathbf{x}_{N-1} | \mathbf{x}_N) d\mathbf{x}_1 \cdots d\mathbf{x}_{N-1} \\ &= \int_{\mathbf{x}_{1:N-1}} \prod_{t=0}^{t=N-1} p_\theta(\mathbf{x}_t | \mathbf{x}_{t+1}, \dots, \mathbf{x}_N) d\mathbf{x}_1 \cdots d\mathbf{x}_{N-1} \\ &= \int_{\mathbf{x}_{1:N-1}} \prod_{t=0}^{t=N-1} p_\theta(\mathbf{x}_t | \mathbf{x}_{t+1}, \mathbf{x}_N) d\mathbf{x}_1 \cdots d\mathbf{x}_{N-1}. \end{aligned} \quad (9)$$

Here, Eq. (8) is utilized in the third equation. The subscript $1 : N - 1$ in the notation $\mathbf{x}_{1:N-1}$ is an abbreviation for $\{\mathbf{x}_1, \dots, \mathbf{x}_{N-1}\}$. For the sake of convenience, we continue to use this abbreviation in the rest of this paper. Equation (9) indicates that we realize the sampling of $q(\mathbf{x}_0 | \mathbf{x}_N)$ through iterative sampling of $p_\theta(\mathbf{x}_t | \mathbf{x}_{t+1}, \mathbf{x}_N)$. Therefore, we have the following sampling algorithm.

Algorithm 1 The general sampling process

Input: noisy image \mathbf{x}_N and model p_θ .

Output: \mathbf{x}_0 .

```

1: for  $t = N - 1, \dots, 0$  do
2:   Sample  $\mathbf{x}_t$  by  $p_\theta(\mathbf{x}_t | \mathbf{x}_{t+1}, \mathbf{x}_N)$ .
3: end for
```

3.1.3 Derivation of Model Training

In fact, $p_\theta(\mathbf{x}_0 | \mathbf{x}_N)$ is a multiple-hidden-variable model with $\mathbf{x}_t, t = 1, \dots, N - 1$. Based on the definition of the

diffusion process and reverse process, we can derive the evidence lower bound objective (ELBO) as follows:

$$\begin{aligned} L &= \mathbb{E}_{\mathbf{x}_0, \mathbf{x}_N} [-\log p_\theta(\mathbf{x}_0 | \mathbf{x}_N)] \\ &\leq \mathbb{E}_{q_{0:N}} \left[-\log \frac{p_\theta(\mathbf{x}_{0:N-1} | \mathbf{x}_N)}{q(\mathbf{x}_{1:N-1} | \mathbf{x}_0, \mathbf{x}_N)} \right] \\ &= \mathbb{E}_{q_{0:N}} \left[-\log \frac{\prod_{t=0}^{t=N-1} p_\theta(\mathbf{x}_t | \mathbf{x}_{t+1}, \mathbf{x}_N)}{q(\mathbf{x}_{1:N-1} | \mathbf{x}_0, \mathbf{x}_N)} \right]. \end{aligned} \quad (10)$$

The proof is in Appendix. The further derivation of Eq. (10) depends on the assumption of diffusion process and will be shown in Sec. 3.2.

3.2. Application

In this part, we discuss three types of noise models for image denoising, Gaussian, Gamma and Poisson noise, as examples. We will give the specific assumption for the diffusion process, derive the objective loss function for training, and show the full sampling algorithms.

3.2.1 Gaussian Noise

The Gaussian noise model in denoising task is defined by the following form:

$$\mathbf{x}_N = \mathbf{x}_0 + \sigma \mathbf{z}, \quad \mathbf{z} \sim \mathcal{N}(\mathbf{0}, \mathbf{I}), \quad (11)$$

where $\mathcal{N}(\mathbf{0}, \mathbf{I})$ is standard Gaussian distribution with independent components.

We select $0 = \sigma_0 < \sigma_1 < \sigma_2 < \dots < \sigma_{N-1} < \sigma_N = \sigma$. Therefore, $\{\sigma_t\}$ is a monotonically increasing sequence. Let

$$\mathbf{x}_{t+1} = \mathbf{x}_t + \sqrt{\sigma_{t+1}^2 - \sigma_t^2} \mathbf{z}_{t+1}, \quad \mathbf{z}_{t+1} \sim \mathcal{N}(\mathbf{0}, \mathbf{I}), \quad (12)$$

where $t = 0, 1, \dots, N - 1$. Then we have:

$$\begin{aligned} \mathbf{x}_t &= \mathbf{x}_0 + \left(\sum_{i=0}^{t-1} \sqrt{\sigma_{i+1}^2 - \sigma_i^2} \mathbf{z}_i \right) \\ &= \mathbf{x}_0 + \sigma_t \mathbf{z}, \quad \mathbf{z} \sim \mathcal{N}(\mathbf{0}, \mathbf{I}), \end{aligned} \quad (13)$$

where $t = 1, \dots, N$. Equation (12) defines the relation between $\mathbf{x}_t, t = 1, \dots, N$ and we have

$$q(\mathbf{x}_t | \mathbf{x}_{0:t-1}) = q(\mathbf{x}_t | \mathbf{x}_{t-1}). \quad (14)$$

Thus, $\mathbf{x}_t, t = 1, \dots, N$ are a Markov chain. By now, we define a full diffusion process for Gaussian Noise.

From Eq. (14), we can derive the following two properties:

$$q(\mathbf{x}_{1:N-1} | \mathbf{x}_0, \mathbf{x}_N) = \prod_{t=1}^{N-1} q(\mathbf{x}_t | \mathbf{x}_0, \mathbf{x}_{t+1}). \quad (15)$$

$$q(\mathbf{x}_t | \mathbf{x}_{t+1:N}) = q(\mathbf{x}_t | \mathbf{x}_{t+1}). \quad (16)$$

The proof of Eq. (15) and Eq. (16) are in Appendix.

Applying Eq. (15) to Eq. (10), we have that:

$$\begin{aligned} L &\leq \mathbb{E}_{q_{0:N}} \left[-\log \frac{\prod_{t=0}^{N-1} p_\theta(\mathbf{x}_t | \mathbf{x}_{t+1}, \mathbf{x}_N)}{\prod_{t=1}^{N-1} q(\mathbf{x}_t | \mathbf{x}_0, \mathbf{x}_{t+1})} \right] \\ &= \mathbb{E}_{q_{0:N}} \left[-\sum_{t=1}^{N-1} \log \frac{p_\theta(\mathbf{x}_t | \mathbf{x}_{t+1}, \mathbf{x}_N)}{q(\mathbf{x}_t | \mathbf{x}_0, \mathbf{x}_{t+1})} - \log p_\theta(\mathbf{x}_0 | \mathbf{x}_1, \mathbf{x}_N) \right] \\ &= \sum_{t=1}^{N-1} \mathbb{E}_{q_{0,t+1,N}} [D_{\text{KL}}(q(\mathbf{x}_t | \mathbf{x}_0, \mathbf{x}_{t+1}) \| p_\theta(\mathbf{x}_t | \mathbf{x}_{t+1}, \mathbf{x}_N))] \\ &\quad + \mathbb{E}_{q_{0,1,N}} [-\log p_\theta(\mathbf{x}_0 | \mathbf{x}_1, \mathbf{x}_N)]. \end{aligned} \quad (17)$$

Because Eq. (16) indicates that given \mathbf{x}_{t+1} , \mathbf{x}_t is not dependent on \mathbf{x}_N when $t < N-1$. Therefore, we can further assume that

$$p_\theta(\mathbf{x}_t | \mathbf{x}_{t+1}, \mathbf{x}_N) = p_\theta(\mathbf{x}_t | \mathbf{x}_{t+1}). \quad (18)$$

As a result, Eq. (17) is simplified as

$$\begin{aligned} L &\leq \sum_{t=1}^{N-1} \mathbb{E}_{q_{0,t+1,N}} [D_{\text{KL}}(q(\mathbf{x}_t | \mathbf{x}_0, \mathbf{x}_{t+1}) \| p_\theta(\mathbf{x}_t | \mathbf{x}_{t+1}))] \\ &\quad + \mathbb{E}_{q_{0,1,N}} [-\log p_\theta(\mathbf{x}_0 | \mathbf{x}_1)]. \end{aligned} \quad (19)$$

Now, we consider the main part of the loss function $\mathbb{E}_{q_{0,t+1,N}} [D_{\text{KL}}(q(\mathbf{x}_t | \mathbf{x}_0, \mathbf{x}_{t+1}) \| p_\theta(\mathbf{x}_t | \mathbf{x}_{t+1}))]$. We begin with the analytical form of $q(\mathbf{x}_t | \mathbf{x}_0, \mathbf{x}_{t+1})$. We have the conclusion that:

$$q(\mathbf{x}_t | \mathbf{x}_0, \mathbf{x}_{t+1}) \sim \mathcal{N}(\tilde{\mu}_t, \tilde{\sigma}_t \mathbf{I}), t = 0, 1, \dots, N-1, \quad (20)$$

where

$$\begin{aligned} \tilde{\mu}_t &= \frac{\sigma_t^2}{\sigma_{t+1}^2} \mathbf{x}_{t+1} + \frac{\sigma_{t+1}^2 - \sigma_t^2}{\sigma_{t+1}^2} \mathbf{x}_0, \\ \tilde{\sigma}_t &= \frac{\sigma_t}{\sigma_{t+1}} \sqrt{\sigma_{t+1}^2 - \sigma_t^2}. \end{aligned} \quad (21)$$

Therefore, we assume that $p_\theta(\mathbf{x}_t | \mathbf{x}_{t+1})$, $t = 1, \dots, N-1$, also follows a Gaussian distribution:

$$p_\theta(\mathbf{x}_t | \mathbf{x}_{t+1}) \sim \mathcal{N}(\mu_{\theta,t+1}(\mathbf{x}_{t+1}), \tilde{\sigma}_t \mathbf{I}), \quad (22)$$

where

$$\mu_{\theta,t+1}(\mathbf{x}_{t+1}) = \frac{\sigma_t^2}{\sigma_{t+1}^2} \mathbf{x}_{t+1} + \frac{\sigma_{t+1}^2 - \sigma_t^2}{\sigma_{t+1}^2} f(\mathbf{x}_{t+1}, t+1; \theta). \quad (23)$$

Algorithm 2 The training process for Gaussian noise

Input: $\{\mathbf{x}_0\}, \{\sigma_t\}, f(\cdot, \cdot, \theta)$.

Output: trained $f(\cdot, \cdot, \theta)$.

```

1: while  $\theta$  is not converged do
2:   Random select  $\mathbf{x}_0$  and sample  $t$  from  $\{1, \dots, N\}$  uniformly.
3:   Sample  $\mathbf{x}_t$  from  $\mathcal{N}(\mathbf{x}_0, \sigma_t^2 \mathbf{I})$ .
4:   Compute grad by  $\nabla_\theta \|f(\mathbf{x}_t, t; \theta) - \mathbf{x}_0\|_2^2$ .
5:   Update  $\theta$  by grad.
6: end while

```

Algorithm 3 The sampling process for Gaussian noise

Input: noisy image \mathbf{x}_N and trained $f(\cdot, \cdot, \theta)$.

Output: \mathbf{x}_0 .

```

1: for  $t = N-1, \dots, 1$  do
2:   Sample  $\mathbf{x}_t$  by

```

$$\mathcal{N}\left(\frac{\sigma_t^2}{\sigma_{t+1}^2} \mathbf{x}_{t+1} + \frac{\sigma_{t+1}^2 - \sigma_t^2}{\sigma_{t+1}^2} f(\mathbf{x}_{t+1}, t+1; \theta), \tilde{\sigma}_t \mathbf{I}\right). \quad (27)$$

```

3: end for

```

```

4:  $\mathbf{x}_0 = f(\mathbf{x}_1, 1, \theta)$ 

```

Here, $f(\mathbf{x}_{t+1}, t+1; \theta)$ is a neural network with input of $(\mathbf{x}_{t+1}, t+1)$. Since $q(\mathbf{x}_t | \mathbf{x}_0, \mathbf{x}_{t+1})$ and $p_\theta(\mathbf{x}_t | \mathbf{x}_{t+1})$ have the same covariance matrix, we can derive that

$$\begin{aligned} D_{\text{KL}}(q(\mathbf{x}_t | \mathbf{x}_0, \mathbf{x}_{t+1}) \| p_\theta(\mathbf{x}_t | \mathbf{x}_{t+1})) \\ = \|\mu_{\theta,t+1}(\mathbf{x}_{t+1}) - \tilde{\mu}_t\|_2^2. \end{aligned} \quad (24)$$

Neglecting the constant coefficient, minimizing Eq. (24) is equivalent to minimize

$$\|f(\mathbf{x}_{t+1}, t+1; \theta) - \mathbf{x}_0\|_2^2 \quad (25)$$

Next, we turn to $\mathbb{E}_{q_{0,1,N}} [-\log p_\theta(\mathbf{x}_0 | \mathbf{x}_1)]$, the last term in Eq. (19). If we assume $p_\theta(\mathbf{x}_0 | \mathbf{x}_1)$ follows some distribution, sampling from it may introduce extra undesired noise. Hence, practically we replace the sampling by $\mathbb{E}[\mathbf{x}_0 | \mathbf{x}_1]$. As a result, we train p_θ by $\mathbb{E}_{q_{0,1,N}} [\|f(\mathbf{x}_1, 1; \theta) - \mathbf{x}_0\|_2^2]$ instead of $\mathbb{E}_{q_{0,1,N}} [-\log p_\theta(\mathbf{x}_0 | \mathbf{x}_1)]$.

Combining with the above analysis, we give the final objective loss function as follows:

$$L = \mathbb{E}_q \sum_{t=0}^{N-1} \|f(\mathbf{x}_{t+1}, t+1; \theta) - \mathbf{x}_0\|_2^2. \quad (26)$$

At last, we show the full training and sampling algorithms in Algorithm 2 and Algorithm 3.

3.2.2 Gamma Noise

The Gamma noise model in denoising task is defined by the following form:

$$\mathbf{x}_N = \boldsymbol{\eta} \odot \mathbf{x}_0, \eta_i \sim \frac{1}{\alpha} \mathcal{G}(\alpha, 1), \quad (28)$$

where $\alpha > 1$ and $\mathcal{G}(\alpha, 1)$ is a Gamma distribution with parameters of α and 1. \odot represents component-wise multiplication. For the sake of convenience, we neglect it in notation if not ambiguous.

We select $\alpha_0 = \infty > \alpha_1 > \dots > \alpha_N = \alpha$. Therefore, $\{\alpha_t\}$ is a monotonically decreasing sequence. Let

$$\mathbf{x}_1 = \boldsymbol{\eta}_1 \mathbf{x}_0, \quad \eta_{1,i} \sim \frac{1}{\alpha_1} \mathcal{G}(\alpha_1, 1), \quad (29)$$

and

$$\mathbf{x}_{t+1} = \frac{\alpha_t}{\alpha_{t+1}} \zeta_{t+1} \mathbf{x}_t, \zeta_{t+1,i} \sim \mathcal{B}(\alpha_{t+1}, \alpha_t - \alpha_{t+1}) \quad (30)$$

where $t = 1, \dots, N-1$ and $\mathcal{B}(\alpha_{t+1}, \alpha_t - \alpha_{t+1})$ is a Beta distribution with parameters of α_{t+1} and $\alpha_t - \alpha_{t+1}$. Then we have:

$$\mathbf{x}_t = \boldsymbol{\eta}_t \mathbf{x}_0, \quad \eta_{t,i} \sim \frac{1}{\alpha_t} \mathcal{G}(\alpha_t, 1), \quad (31)$$

where $t = 0, 1, \dots, N-1$. The proof of Eq. (31) is in Appendix. Equation (30) define the relation between \mathbf{x}_t , $t = 1, \dots, N$. By now, we define a full diffusion process for Gamma Noise. Obviously, Eq. (14) holds according to Eq. (30). Thus, \mathbf{x}_t , $t = 1, \dots, N$ are also a Markov chain.

Based on the analysis in Sec. 3.2.1, we know that all the equations from Eq. (15) to Eq. (19) still hold.

Now, we consider the main part of the loss function $\mathbb{E}_{q_{0,t+1,N}} [D_{\text{KL}}(q(\mathbf{x}_t | \mathbf{x}_0, \mathbf{x}_{t+1}) \| p_\theta(\mathbf{x}_t | \mathbf{x}_{t+1}))]$. We begin with the analytical form of $q(\mathbf{x}_t | \mathbf{x}_0, \mathbf{x}_{t+1})$. We have the conclusion that:

$$\left(\frac{\alpha_t \mathbf{x}_t - \alpha_{t+1} \mathbf{x}_{t+1}}{\mathbf{x}_0} \right)_i \sim \mathcal{G}(\alpha_t - \alpha_{t+1}, 1), t = 1, \dots, N-1. \quad (32)$$

Here, the division is component-wise operation. Thus, $q(\mathbf{x}_t | \mathbf{x}_0, \mathbf{x}_{t+1})$ can be represented by

$$\mathbf{x}_t = \frac{\mathbf{x}_0 \boldsymbol{\tau}_t + \alpha_{t+1} \mathbf{x}_{t+1}}{\alpha_t}, \tau_{t,i} \sim \mathcal{G}(\alpha_t - \alpha_{t+1}, 1). \quad (33)$$

Therefore, we assume that $p_\theta(\mathbf{x}_t | \mathbf{x}_{t+1})$, $t = 1, \dots, N-1$ has the following form:

$$\mathbf{x}_t = \frac{f(\mathbf{x}_{t+1}, t+1; \theta) \boldsymbol{\tau}_t + \alpha_{t+1} \mathbf{x}_{t+1}}{\alpha_t}, \tau_{t,i} \sim \mathcal{G}(\alpha_t - \alpha_{t+1}, 1) \quad (34)$$

Algorithm 4 The training process for Gamma noise

Input: $\{\mathbf{x}_0\}, \{\alpha_t\}, f(\cdot, \cdot, \theta)$.

Output: trained $f(\cdot, \cdot, \theta)$.

- 1: **while** θ is not converged **do**
 - 2: Random select \mathbf{x}_0 and sample t from $\{1, \dots, N\}$ uniformly.
 - 3: Sample $\boldsymbol{\eta}_t$ from $\mathcal{G}(\alpha_t, 1)$
 - 4: $\mathbf{x}_t = \boldsymbol{\eta}_t \mathbf{x}_0$.
 - 5: Compute grad by $\nabla_\theta \|f(\mathbf{x}_t, t; \theta) - \mathbf{x}_0\|_2^2$.
 - 6: Update θ by grad.
 - 7: **end while**
-

Algorithm 5 The sampling process for Gamma noise

Input: noisy image \mathbf{x}_N , $\{\alpha_t\}$, and trained $f(\cdot, \cdot, \theta)$.

Output: \mathbf{x}_0 .

- 1: **for** $t = N-1, \dots, 1$ **do**
 - 2: Sample $\boldsymbol{\tau}_t$ from $\mathcal{G}(\alpha_t - \alpha_{t+1}, 1)$.
 - 3: $\mathbf{x}_t = \frac{1}{\alpha_t} (f(\mathbf{x}_{t+1}, t+1; \theta) \boldsymbol{\tau}_t + \alpha_{t+1} \mathbf{x}_{t+1})$
 - 4: **end for**
 - 5: $\mathbf{x}_0 = f(\mathbf{x}_1, 1, \theta)$
-

where $f(\mathbf{x}_{t+1}, t+1; \theta)$ is a neural network with input of $(\mathbf{x}_{t+1}, t+1)$. Then we can derive that

$$\begin{aligned} & D_{\text{KL}}(q(\mathbf{x}_t | \mathbf{x}_0, \mathbf{x}_{t+1}) \| p_\theta(\mathbf{x}_t | \mathbf{x}_{t+1})) \\ &= \sum_i (\alpha_t - \alpha_{t+1}) \left(\log \frac{f_{\theta,i}}{\mathbf{x}_0} + \frac{\mathbf{x}_0}{f_{\theta,i}} - 1 \right). \end{aligned} \quad (35)$$

Here, f_θ is the abbreviation of $f(\mathbf{x}_{t+1}, t+1; \theta)$. Suppose f_{θ^*} is the optimal function minimizing Eq. (35), we can prove that it is also the optimal function for the following optimization problem:

$$\min_{f_\theta} \mathbb{E}_q \|f(\mathbf{x}_{t+1}, t+1; \theta) - \mathbf{x}_0\|_2^2. \quad (36)$$

The proof is in Appendix. Hence, training f_θ by minimize KL divergence is equivalent to train f_θ by L2 norm loss function with \mathbf{x}_0 as labels.

As for $\mathbb{E}_{q_{0,1,N}} [-\log p_\theta(\mathbf{x}_0 | \mathbf{x}_1)]$, the last term in Eq. (19), we adapt the same strategy described in Sec. 3.2.1. As a result, the final objective loss function is as follows:

$$L = \mathbb{E}_q \sum_{t=0}^{t=N-1} \|f(\mathbf{x}_{t+1}, t+1; \theta) - \mathbf{x}_0\|_2^2. \quad (37)$$

At last, we show the full training and sampling algorithms in Algorithm 4 and Algorithm 5.

3.2.3 Poisson Noise

The Poisson noise model in denoising task is defined by the following form:

$$\mathbf{x}_N = \frac{\mathcal{P}(\lambda \mathbf{x}_0)}{\lambda}, \quad (38)$$

where $\lambda > 0$ and $\mathcal{P}(\lambda \mathbf{x}_0)$ is a Poisson distribution with parameters of $\lambda \mathbf{x}_0$.

We select $\infty = \lambda_0 > \lambda_1 > \dots > \lambda_N = \lambda$. Therefore, $\{\lambda_t\}$ is a monotonically decreasing sequence. Let

$$\mathbf{x}_N | \mathbf{x}_0 \sim \frac{\mathcal{P}(\lambda_N \mathbf{x}_0)}{\lambda_N}, \quad (39)$$

and

$$\mathbf{x}_t | \mathbf{x}_{t+1}, \mathbf{x}_0 \sim \frac{\lambda_{t+1} \mathbf{x}_{t+1} + \mathcal{P}((\lambda_t - \lambda_{t+1}) \mathbf{x}_0)}{\lambda_t}, \quad (40)$$

where $t = 1, \dots, N-1$. Then we have:

$$\mathbf{x}_t | \mathbf{x}_0 \sim \frac{\mathcal{P}(\lambda_t \mathbf{x}_0)}{\lambda_t}, \quad (41)$$

where $t = 1, \dots, N-1$. The proof of Eq. (41) is in Appendix. Equation (40) define the relation between \mathbf{x}_t , $t = 1, \dots, N$. by now, we define a full diffusion process for Poisson Noise. According to Eq. (40), we have

$$q(\mathbf{x}_t | \mathbf{x}_0, \mathbf{x}_{t+1:N}) = q(\mathbf{x}_t | \mathbf{x}_0, \mathbf{x}_{t+1}). \quad (42)$$

From Eq. (42), we can derive that

$$\begin{aligned} q(\mathbf{x}_{1:N-1} | \mathbf{x}_0, \mathbf{x}_N) &= \prod_{t=1}^{N-1} q(\mathbf{x}_t | \mathbf{x}_0, \mathbf{x}_{t+1:N}) \\ &= \prod_{t=1}^{N-1} q(\mathbf{x}_t | \mathbf{x}_0, \mathbf{x}_{t+1}). \end{aligned} \quad (43)$$

Applying Eq. (43) to Eq. (10), we can derive the same result as Eq. (17):

$$\begin{aligned} L &\leq \sum_{t=1}^{N-1} \mathbb{E}_{q_{0,t+1,N}} [D_{\text{KL}}(q(\mathbf{x}_t | \mathbf{x}_0, \mathbf{x}_{t+1}) \| p_{\theta}(\mathbf{x}_t | \mathbf{x}_{t+1}, \mathbf{x}_N))] \\ &\quad + \mathbb{E}_{q_{0,1,N}} [-\log p_{\theta}(\mathbf{x}_0 | \mathbf{x}_1, \mathbf{x}_N)]. \end{aligned} \quad (44)$$

However, \mathbf{x}_N in $p_{\theta}(\mathbf{x}_t | \mathbf{x}_{t+1}, \mathbf{x}_N)$ cannot be removed. Thus, Eq. (19) does not hold for Poisson noise model.

Now, we consider the main part of the loss function $\mathbb{E}_{q_{0,t+1,N}} [D_{\text{KL}}(q(\mathbf{x}_t | \mathbf{x}_0, \mathbf{x}_{t+1}) \| p_{\theta}(\mathbf{x}_t | \mathbf{x}_{t+1}))]$. We have known the analytical form of $q(\mathbf{x}_t | \mathbf{x}_0, \mathbf{x}_{t+1})$ from Eq. (40). Therefore, we assume that $p_{\theta}(\mathbf{x}_t | \mathbf{x}_{t+1}, \mathbf{x}_0)$, $t = 1, \dots, N-1$ has the following form:

$$\begin{aligned} p_{\theta}(\mathbf{x}_t | \mathbf{x}_{t+1}, \mathbf{x}_N) \\ \sim \frac{\lambda_{t+1} \mathbf{x}_{t+1} + \mathcal{P}((\lambda_t - \lambda_{t+1}) f(\mathbf{x}_{t+1}, \mathbf{x}_N, t+1; \theta))}{\lambda_t}, \end{aligned} \quad (45)$$

where $f(\mathbf{x}_{t+1}, \mathbf{x}_N, t+1; \theta)$ is a neural network with input of $(\mathbf{x}_{t+1}, \mathbf{x}_N, t+1)$. Denote $f(\mathbf{x}_{t+1}, \mathbf{x}_N, t+1; \theta)$ as f_{θ}

Algorithm 6 The training process for Poisson noise

Input: $\{\mathbf{x}_0\}, \{\lambda_t\}, f(\cdot, \cdot, \theta)$.

Output: trained $f(\cdot, \cdot, \theta)$.

- 1: **while** θ is not converged **do**
 - 2: Random select \mathbf{x}_0 and sample t from $\{1, \dots, N-1\}$ uniformly.
 - 3: Sample \mathbf{x}_N from $\frac{\mathcal{P}(\lambda_N \mathbf{x}_0)}{\lambda_N}$.
 - 4: Sample \mathbf{x}_t from $\frac{1}{\lambda_t} (\lambda_{t+1} \mathbf{x}_{t+1} + \mathcal{P}((\lambda_t - \lambda_{t+1}) \mathbf{x}_0))$
 - 5: Compute grad by $\nabla_{\theta} \|f(\mathbf{x}_t, \mathbf{x}_N, t; \theta) - \mathbf{x}_0\|_2^2$.
 - 6: Update θ by grad.
 - 7: **end while**
-

Algorithm 7 The sampling process for Poisson noise

Input: noisy image \mathbf{x}_N , $\{\lambda_t\}$ and trained $f(\cdot, \cdot, \theta)$.

Output: \mathbf{x}_0 .

- 1: **for** $t = N-1, \dots, 1$ **do**
 - 2: Sample τ_t from $\mathcal{P}((\lambda_t - \lambda_{t+1}) f(\mathbf{x}_{t+1}, \mathbf{x}_N, t; \theta))$
 - 3: $\mathbf{x}_t = \frac{1}{\lambda_t} (\lambda_{t+1} \mathbf{x}_{t+1} + \tau_t)$
 - 4: **end for**
 - 5: $\mathbf{x}_0 = f(\mathbf{x}_1, \mathbf{x}_N, 1, \theta)$
-

for simplicity, then we can derive that

$$\begin{aligned} D_{\text{KL}}(q(\mathbf{x}_t | \mathbf{x}_0, \mathbf{x}_{t+1}) \| p_{\theta}(\mathbf{x}_t | \mathbf{x}_{t+1}, \mathbf{x}_N)) \\ = (\log \mathbf{x}_0 - \log f_{\theta})(\lambda_t - \lambda_{t+1}) \mathbf{x}_0 \\ - (\lambda_t - \lambda_{t+1})(\mathbf{x}_0 - f_{\theta}). \end{aligned} \quad (46)$$

Similar to the analysis in Sec. 3.2.2, we attempt to transform the original optimization problem to another equivalent one. Suppose f_{θ^*} is the optimal function minimizing Eq. (46), we can prove that it is also the optimal function for the following optimization problem:

$$\min_{f_{\theta}} \mathbb{E}_q \|f(\mathbf{x}_{t+1}, \mathbf{x}_N, t+1; \theta) - \mathbf{x}_0\|_2^2. \quad (47)$$

The proof is in Appendix. Hence, training f_{θ} by minimize KL divergence is equivalent to train f_{θ} by L2 norm loss function with \mathbf{x}_0 as labels.

As for $\mathbb{E}_{q_{0,1,N}} [-\log p_{\theta}(\mathbf{x}_0 | \mathbf{x}_1, \mathbf{x}_N)]$, the last term in Eq. (44), we still adapt the same strategy described in Sec. 3.2.1. As a result, the final objective loss function is as follows:

$$L = \mathbb{E}_q \sum_{t=0}^{t=N-1} \|f(\mathbf{x}_{t+1}, \mathbf{x}_N, t+1; \theta) - \mathbf{x}_0\|_2^2. \quad (48)$$

At last, we show the full training and sampling algorithms in Algorithm 6 and Algorithm 7.

3.3. Discussion

In this section, we have discussed three types of noise models in the denoising task, Gaussian, Gamma and Pois-

son noise. The diffusion process of Gaussian and Gamma noise can be defined as a Markov chain, representing the evolution from clean images to noisy images. Gaussian distribution itself is additive. Thus, its diffusion process is only related to Gaussian distribution. While Beta distribution is introduced to define the diffusion process for Gamma noise. As for Poisson noise, the difference is clear. From definition, its diffusion process can also be regarded as another form of Markov chain, which is conditioned on \mathbf{x}_0 and represents an evolution from noisier images to less noisy images. Hence, the definition of diffusion process is related to the statistical property of the noise model.

About the derivation of objective loss functions of model training, the basic idea is to minimize KL divergence. In the case of Gamma noise and Poisson noise, we transform the original complex optimization problem to L2 norm loss minimization through optimization equivalence. As a result, the model training for three noise models are highly consistent. Though the input of models are slightly different, they can all be written as

$$\min \mathbb{E}_{q,t} \|f_{\theta,t} - \mathbf{x}_0\|_2^2. \quad (49)$$

In other words, given t the model training amounts to estimate the posterior mean, $\mathbb{E}[\mathbf{x}_0 | \mathbf{x}_{t+1}, \mathbf{x}_N]$. Therefore, $p_{\theta}(\mathbf{x}_t | \mathbf{x}_{t+1}, \mathbf{x}_N)$ is constructed through replacing the \mathbf{x}_0 in $q(\mathbf{x}_t | \mathbf{x}_0, \mathbf{x}_{t+1})$ by the posterior mean.

4. Experiment

We conduct extensive experiments to evaluate our approach, including Gaussian noise, Gamma noise and Poisson noise with different noise levels.

Dataset and Implementation Details We evaluate the proposed method for gray images in the two benchmark datasets: KODAK dataset and CSet9. DIV2K [21] and CBSD500 dataset [2] are used as training datasets. Original images are color RGB natural images and we transform them to gray images when training and testing. We use traditional supervised learning (Eq. (2)) with as L2 norm loss as the baseline for comparison. The same modified U-Net [5] with about 70 million parameters is used for all methods. When training, we randomly clip the training images to patches with the resolution of 128×128 . AdamW optimizer [13] is used to train the network. We train each model with the batch size of 32. To reduce memory, we utilize the tricks of cumulative gradient and mixed precision training. The learning rate is set as 1×10^{-4} . All the models are implemented in PyTorch [15] with NVidia V100. The pixel value range of all clean images are $[0, 255]$ and the parameters of noise models are built on it. When training models, images will be scaled to $[-1, 1]$. After generating samples, they will be scaled back to $[0, 255]$. For each

type of noise model, we choose two noise level and different number of diffusion steps, N . We list them here:

- Gaussian: $\sigma = 25$ ($N = 20$), $\sigma = 50$ ($N = 40$);
- Gamma: $\alpha = 26$ ($N = 20$), $\alpha = 6.5$ ($N = 40$);
- Poisson: $\lambda = 0.2$ ($N = 20$), $\lambda = 0.1$ ($N = 40$).

Another setting which is not discussed in Sec. 3 is how to construct the sequence of noise model parameters. In our experiments, we adapt a simple but effective way in which the sequence is constructed such that the standard deviation of $\mathbf{x}_t | \mathbf{x}_0$ is linearly increased from $t = 0$ to $t = N$. The more details of implementation are described in Appendix.

Results Figure 3 shows the generated samples for different noise models. Compared to supervised learning, our generated results are visually pleasing, containing better image details. The good visual quality of generated samples verifies that our method is feasible for generative denoising tasks. We also compute the PSNR and SSIM to evaluate our method as shown in Tab. 1. We discover that there is a gap between supervised learning and generated samples in terms of metrics. This is understandable. Because noisy images have lost much original image information, it is hard to generate completely identical details to those lost ones. For each noisy images, we generate 100 samples and compute the mean of them as the estimation of $p(\mathbf{x} | \mathbf{y})$, which are also illustrated in Tab. 1. Apparently, the metrics of sample mean is close to supervised learning, which further verifies that the posterior distribution estimated by our method is effective. We also investigate the effect of the number of steps, N . Due to the limit of paper length, we discuss it in Appendix.

5. Conclusion

In this paper, we apply the framework of diffusion models to generative image denoising tasks and propose a new diffusion model based on the image noise model. Different to the original diffusion model, we redefine the diffusion process according to the specific noise models and derive the model training and sampling algorithms. Interestingly, we find that model training for Gaussian, Gamma and Poisson noise is unified to a highly consistent strategy. Our experiments verify that our method is feasible for generative image denoising. In the future, we hope to extend our method to other noise model and evaluate its performance on other dataset.

References

- [1] Saeed Anwar and Nick Barnes. Real image denoising with feature attention. In *Proceedings of the*

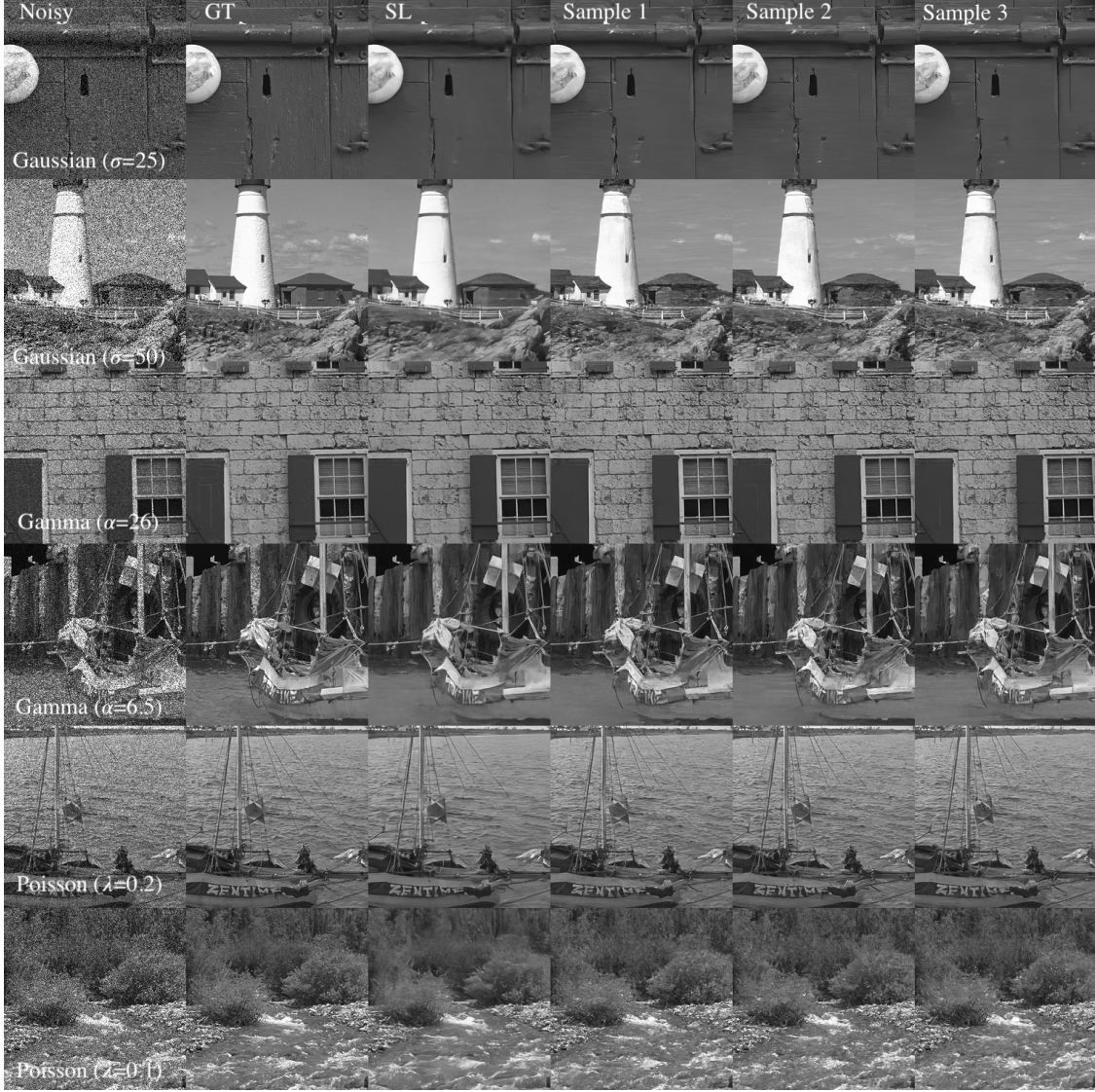


Figure 3. Qualitative comparison using Kodak dataset. From top to bottom is: Gaussian noise with $\sigma = 25$ and $\sigma = 50$, Gamma noise with $\alpha = 26$ and $\alpha = 6.5$, and Poisson noise with $\lambda = 0.2$ and $\lambda = 0.1$. Noisy: noisy image, GT: ground-truth, SL: supervised learning. The last three columns are generated different samples.

Noise Model	Kodak			CSet9		
	SL	Samples	Mean of Samples	SL	Samples	Mean of Samples
Gaussian, $\sigma = 25$	30.53 / 0.816	28.38 / 0.755	30.45 / 0.820	29.41 / 0.843	27.35 / 0.792	29.41 / 0.849
Gaussian, $\sigma = 50$	27.69 / 0.742	25.30 / 0.645	27.63 / 0.742	26.11 / 0.760	23.69 / 0.664	26.26 / 0.766
Gamma, $\alpha = 26$	31.18 / 0.849	28.59 / 0.789	30.84 / 0.852	29.68 / 0.854	27.55 / 0.807	29.64 / 0.859
Gamma, $\alpha = 6.5$	28.31 / 0.776	26.40 / 0.710	28.23 / 0.775	26.52 / 0.776	24.51 / 0.712	26.62 / 0.781
Poisson, $\lambda = 0.2$	30.95 / 0.834	28.71 / 0.770	30.76 / 0.834	29.68 / 0.851	27.53 / 0.782	29.69 / 0.851
Poisson, $\lambda = 0.1$	29.31 / 0.794	26.96 / 0.696	29.28 / 0.792	27.88 / 0.810	25.53 / 0.706	27.97 / 0.810

Table 1. Quantitative comparison in terms of PSNR (dB) / SSIM for different noise model on Kodak and CSet9 datasets. We compare supervised learning (SL) to our method. "Samples" means the generated results while "Mean of Samples" means the average of 100 samples for each noisy images.

- IEEE/CVF international conference on computer vision*, pages 3155–3164, 2019. 2
- [2] Lalit Chaudhary and Yogesh Yogesh. A comparative study of fruit defect segmentation techniques. In *2019 International Conference on Issues and Challenges in Intelligent Computing Techniques (ICICT)*, volume 1, pages 1–4. IEEE, 2019. 7
- [3] Shen Cheng, Yuzhi Wang, Haibin Huang, Donghao Liu, Haoqiang Fan, and Shuaicheng Liu. Nbnnet: Noise basis learning for image denoising with subspace projection. In *Proceedings of the IEEE/CVF Conference on Computer Vision and Pattern Recognition*, pages 4896–4906, 2021. 2
- [4] Kostadin Dabov, Alessandro Foi, Vladimir Katkovnik, and Karen Egiazarian. Image denoising with block-matching and 3d filtering. In *Image processing: algorithms and systems, neural networks, and machine learning*, volume 6064, pages 354–365. SPIE, 2006. 1
- [5] Prafulla Dhariwal and Alexander Nichol. Diffusion models beat gans on image synthesis. *Advances in Neural Information Processing Systems*, 34:8780–8794, 2021. 7
- [6] Shi Guo, Zifei Yan, Kai Zhang, Wangmeng Zuo, and Lei Zhang. Toward convolutional blind denoising of real photographs. In *Proceedings of the IEEE/CVF conference on computer vision and pattern recognition*, pages 1712–1722, 2019. 2
- [7] Jonathan Ho, Ajay Jain, and Pieter Abbeel. Denoising diffusion probabilistic models. *arXiv preprint arXiv:2006.11239*, 2020. 1, 2
- [8] Xiaowan Hu, Ruijun Ma, Zhihong Liu, Yuanhao Cai, Xiaole Zhao, Yulun Zhang, and Haoqian Wang. Pseudo 3d auto-correlation network for real image denoising. In *Proceedings of the IEEE/CVF Conference on Computer Vision and Pattern Recognition*, pages 16175–16184, 2021. 2
- [9] Yoonsik Kim, Jae Woong Soh, Gu Yong Park, and Nam Ik Cho. Transfer learning from synthetic to real-noise denoising with adaptive instance normalization. In *Proceedings of the IEEE/CVF Conference on Computer Vision and Pattern Recognition*, pages 3482–3492, 2020. 2
- [10] Zhifeng Kong, Wei Ping, Jiaji Huang, Kexin Zhao, and Bryan Catanzaro. Diffwave: A versatile diffusion model for audio synthesis. *arXiv preprint arXiv:2009.09761*, 2020. 1
- [11] Yao Li, Xueyang Fu, and Zheng-Jun Zha. Cross-patch graph convolutional network for image denoising. In *Proceedings of the IEEE/CVF International Conference on Computer Vision*, pages 4651–4660, 2021. 2
- [12] Yang Liu, Zhenyue Qin, Saeed Anwar, Pan Ji, Dongwoo Kim, Sabrina Caldwell, and Tom Gedeon. Invertible denoising network: A light solution for real noise removal. In *Proceedings of the IEEE/CVF conference on computer vision and pattern recognition*, pages 13365–13374, 2021. 2
- [13] Ilya Loshchilov and Frank Hutter. Decoupled weight decay regularization. *arXiv preprint arXiv:1711.05101*, 2017. 7
- [14] Chenlin Meng, Yang Song, Jiaming Song, Jiajun Wu, Jun-Yan Zhu, and Stefano Ermon. Sdedit: Image synthesis and editing with stochastic differential equations. *arXiv preprint arXiv:2108.01073*, 2021. 1
- [15] Adam Paszke, Sam Gross, Soumith Chintala, Gregory Chanan, Edward Yang, Zachary DeVito, Zeming Lin, Alban Desmaison, Luca Antiga, and Adam Lerer. Automatic differentiation in pytorch. 2017. 7
- [16] Sathish Ramani, Thierry Blu, and Michael Unser. Monte-carlo sure: A black-box optimization of regularization parameters for general denoising algorithms. *IEEE Transactions on image processing*, 17(9):1540–1554, 2008. 1
- [17] Chao Ren, Xiaohai He, Chuncheng Wang, and Zhibo Zhao. Adaptive consistency prior based deep network for image denoising. In *proceedings of the IEEE/CVF conference on computer vision and pattern recognition*, pages 8596–8606, 2021. 2
- [18] Chitwan Saharia, Jonathan Ho, William Chan, Tim Salimans, David J Fleet, and Mohammad Norouzi. Image super-resolution via iterative refinement. *arXiv preprint arXiv:2104.07636*, 2021. 1
- [19] Jascha Sohl-Dickstein, Eric Weiss, Niru Maheswaranathan, and Surya Ganguli. Deep unsupervised learning using nonequilibrium thermodynamics. In *International Conference on Machine Learning*, pages 2256–2265. PMLR, 2015. 1
- [20] Yang Song, Jascha Sohl-Dickstein, Diederik P Kingma, Abhishek Kumar, Stefano Ermon, and Ben Poole. Score-based generative modeling through stochastic differential equations. *arXiv preprint arXiv:2011.13456*, 2020. 1
- [21] Radu Timofte, Shuhang Gu, Jiqing Wu, and Luc Van Gool. Ntire 2018 challenge on single image super-resolution: Methods and results. In *Proceedings of the IEEE conference on computer vision and pattern recognition workshops*, pages 852–863, 2018. 7
- [22] Yutong Xie, Dufan Wu, Bin Dong, and Quanzheng Li. Trained model in supervised deep learning is a conditional risk minimizer. *arXiv preprint arXiv:2202.03674*, 2022. 12, 13

- [23] Zongsheng Yue, Hongwei Yong, Qian Zhao, Deyu Meng, and Lei Zhang. Variational denoising network: Toward blind noise modeling and removal. *Advances in neural information processing systems*, 32, 2019. 2
- [24] Syed Waqas Zamir, Aditya Arora, Salman Khan, Munawar Hayat, Fahad Shahbaz Khan, Ming-Hsuan Yang, and Ling Shao. Cycleisp: Real image restoration via improved data synthesis. In *Proceedings of the IEEE/CVF Conference on Computer Vision and Pattern Recognition*, pages 2696–2705, 2020. 2
- [25] Syed Waqas Zamir, Aditya Arora, Salman Khan, Munawar Hayat, Fahad Shahbaz Khan, Ming-Hsuan Yang, and Ling Shao. Learning enriched features for real image restoration and enhancement. In *European Conference on Computer Vision*, pages 492–511. Springer, 2020. 2
- [26] Kai Zhang, Wangmeng Zuo, Yunjin Chen, Deyu Meng, and Lei Zhang. Beyond a gaussian denoiser: Residual learning of deep cnn for image denoising. *IEEE transactions on image processing*, 26(7):3142–3155, 2017. 1, 2
- [27] Kai Zhang, Wangmeng Zuo, and Lei Zhang. Ffdnet: Toward a fast and flexible solution for cnn-based image denoising. *IEEE Transactions on Image Processing*, 27(9):4608–4622, 2018. 2
- [28] Hongyi Zheng, Hongwei Yong, and Lei Zhang. Deep convolutional dictionary learning for image denoising. In *Proceedings of the IEEE/CVF Conference on Computer Vision and Pattern Recognition*, pages 630–641, 2021. 2
- [29] Yuqian Zhou, Jianbo Jiao, Haibin Huang, Yang Wang, Jue Wang, Honghui Shi, and Thomas Huang. When awgn-based denoiser meets real noises. In *Proceedings of the AAAI Conference on Artificial Intelligence*, volume 34, pages 13074–13081, 2020. 2

A. Proofs

A.1. The Proof of Eq. (10) in Sec. 3.1.3

$$L \leq \mathbb{E}_{q_{0:N}} \left[-\log \frac{\prod_{t=0}^{t=N-1} p_{\theta}(\mathbf{x}_t | \mathbf{x}_{t+1}, \mathbf{x}_N)}{q(\mathbf{x}_{1:N-1} | \mathbf{x}_0, \mathbf{x}_N)} \right]. \quad (10)$$

The full derivation is as follows.

Proof.

$$\begin{aligned} L &= \mathbb{E}_{\mathbf{x}_0, \mathbf{x}_N} [-\log p_{\theta}(\mathbf{x}_0 | \mathbf{x}_N)] \\ &= \mathbb{E}_{\mathbf{x}_0, \mathbf{x}_N} \left[-\log \int_{\mathbf{x}_1, \dots, \mathbf{x}_{N-1}} p_{\theta}(\mathbf{x}_0, \mathbf{x}_1, \dots, \mathbf{x}_{N-1} | \mathbf{x}_N) \right. \\ &\quad \left. d\mathbf{x}_1 \cdots d\mathbf{x}_{N-1} \right] \\ &= \mathbb{E}_{\mathbf{x}_0, \mathbf{x}_N} \left[-\log \int_{\mathbf{x}_1, \dots, \mathbf{x}_{N-1}} \frac{p_{\theta}(\mathbf{x}_0, \mathbf{x}_1, \dots, \mathbf{x}_{N-1} | \mathbf{x}_N)}{q(\mathbf{x}_1, \dots, \mathbf{x}_{N-1} | \mathbf{x}_0, \mathbf{x}_N)} \right. \\ &\quad \left. q(\mathbf{x}_1, \dots, \mathbf{x}_{N-1} | \mathbf{x}_0, \mathbf{x}_N) d\mathbf{x}_1 \cdots d\mathbf{x}_{N-1} \right] \\ &\leq \mathbb{E}_{\mathbf{x}_0, \mathbf{x}_N} \left[-\log \int_{\mathbf{x}_1, \dots, \mathbf{x}_{N-1}} q(\mathbf{x}_1, \dots, \mathbf{x}_{N-1} | \mathbf{x}_0, \mathbf{x}_N) \right. \\ &\quad \left. \log \frac{p_{\theta}(\mathbf{x}_0, \mathbf{x}_1, \dots, \mathbf{x}_{N-1} | \mathbf{x}_N)}{q(\mathbf{x}_1, \dots, \mathbf{x}_{N-1} | \mathbf{x}_0, \mathbf{x}_N)} d\mathbf{x}_1 \cdots d\mathbf{x}_{N-1} \right] \\ &= \mathbb{E}_{\mathbf{x}_0, \mathbf{x}_N} \left[\mathbb{E}_{\mathbf{x}_1, \dots, \mathbf{x}_{N-1} | \mathbf{x}_0, \mathbf{x}_N} \left[-\log \frac{p_{\theta}(\mathbf{x}_0, \mathbf{x}_1, \dots, \mathbf{x}_{N-1} | \mathbf{x}_N)}{q(\mathbf{x}_1, \dots, \mathbf{x}_{N-1} | \mathbf{x}_0, \mathbf{x}_N)} \right] \right] \\ &= \mathbb{E}_{\mathbf{x}_0, \mathbf{x}_1, \dots, \mathbf{x}_{N-1}, \mathbf{x}_N} \left[-\log \frac{p_{\theta}(\mathbf{x}_0, \mathbf{x}_1, \dots, \mathbf{x}_{N-1} | \mathbf{x}_N)}{q(\mathbf{x}_1, \dots, \mathbf{x}_{N-1} | \mathbf{x}_0, \mathbf{x}_N)} \right] \\ &= \mathbb{E}_{q_{0:N}} \left[-\log \frac{p_{\theta}(\mathbf{x}_{0:N-1} | \mathbf{x}_N)}{q(\mathbf{x}_{1:N-1} | \mathbf{x}_0, \mathbf{x}_N)} \right]. \end{aligned}$$

□

A.2. The Proof of Eq. (15) in Sec. 3.2.1

$$q(\mathbf{x}_{1:N-1} | \mathbf{x}_0, \mathbf{x}_N) = \prod_{t=1}^{N-1} q(\mathbf{x}_t | \mathbf{x}_0, \mathbf{x}_{t+1}). \quad (15)$$

Proof. According to Eq. (14), we have the following derivation:

$$\begin{aligned} &q(\mathbf{x}_{1:N-1} | \mathbf{x}_0, \mathbf{x}_N) \\ &= \prod_{t=1}^{N-1} q(\mathbf{x}_t | \mathbf{x}_0, \mathbf{x}_{t+1:N}) \\ &= \prod_{t=1}^{N-1} \frac{q(\mathbf{x}_t, \mathbf{x}_{t+2:N} | \mathbf{x}_0, \mathbf{x}_{t+1})}{q(\mathbf{x}_{t+2:N} | \mathbf{x}_0, \mathbf{x}_{t+1})} \\ &= \prod_{t=1}^{N-1} \frac{q(\mathbf{x}_{t+2:N} | \mathbf{x}_0, \mathbf{x}_{t+1}, \mathbf{x}_t) q(\mathbf{x}_t | \mathbf{x}_0, \mathbf{x}_{t+1})}{q(\mathbf{x}_{t+2:N} | \mathbf{x}_0, \mathbf{x}_{t+1})} \\ &= \prod_{t=1}^{N-1} \frac{q(\mathbf{x}_{t+2:N} | \mathbf{x}_{t+1}) q(\mathbf{x}_t | \mathbf{x}_0, \mathbf{x}_{t+1})}{q(\mathbf{x}_{t+2:N} | \mathbf{x}_{t+1})} \\ &= \prod_{t=1}^{N-1} q(\mathbf{x}_t | \mathbf{x}_0, \mathbf{x}_{t+1}). \end{aligned}$$

Equation (14) is applied in the fourth equation.

□

A.3. The Proof of Eq. (16) in Sec. 3.2.1

$$q(\mathbf{x}_t | \mathbf{x}_{t+1:N}) = q(\mathbf{x}_t | \mathbf{x}_{t+1}). \quad (16)$$

Proof.

$$\begin{aligned} & q(\mathbf{x}_t | \mathbf{x}_{t+1:N}) \\ &= \frac{q(\mathbf{x}_t, \mathbf{x}_{t+2:N} | \mathbf{x}_{t+1})}{q(\mathbf{x}_{t+2:N} | \mathbf{x}_{t+1})} \\ &= \frac{q(\mathbf{x}_t | \mathbf{x}_{t+1}) q(\mathbf{x}_{t+2:N} | \mathbf{x}_{t+1}, \mathbf{x}_t)}{q(\mathbf{x}_{t+2:N} | \mathbf{x}_{t+1})} \\ &= \frac{q(\mathbf{x}_t | \mathbf{x}_{t+1}) q(\mathbf{x}_{t+2:N} | \mathbf{x}_{t+1})}{q(\mathbf{x}_{t+2:N} | \mathbf{x}_{t+1})} \\ &= q(\mathbf{x}_t | \mathbf{x}_{t+1}). \end{aligned}$$

Equation (14) is applied in the third equation. \square

A.4. The Proof of Eq. (20) and Eq. (21) in Sec. 3.2.1

$$q(\mathbf{x}_t | \mathbf{x}_0, \mathbf{x}_{t+1}) \sim \mathcal{N}(\tilde{\boldsymbol{\mu}}_t, \tilde{\sigma}_t \mathbf{I}), t = 0, 1, \dots, N-1, \quad (20)$$

where

$$\begin{aligned} \tilde{\boldsymbol{\mu}}_t &= \frac{\sigma_t^2}{\sigma_{t+1}^2} \mathbf{x}_{t+1} + \frac{\sigma_{t+1}^2 - \sigma_t^2}{\sigma_{t+1}^2} \mathbf{x}_0, \\ \tilde{\sigma}_t &= \frac{\sigma_t}{\sigma_{t+1}} \sqrt{\sigma_{t+1}^2 - \sigma_t^2}. \end{aligned} \quad (21)$$

Proof. Firstly, we have the following derivation according to Bayesian Equation.

$$\begin{aligned} q(\mathbf{x}_t | \mathbf{x}_0, \mathbf{x}_{t+1}) &= \frac{q(\mathbf{x}_t, \mathbf{x}_{t+1} | \mathbf{x}_0)}{q(\mathbf{x}_{t+1} | \mathbf{x}_0)} \\ &= \frac{q(\mathbf{x}_t | \mathbf{x}_0) q(\mathbf{x}_{t+1} | \mathbf{x}_t)}{q(\mathbf{x}_{t+1} | \mathbf{x}_0)}. \end{aligned}$$

Since $q(\mathbf{x}_t | \mathbf{x}_0)$, $q(\mathbf{x}_{t+1} | \mathbf{x}_t)$ and $q(\mathbf{x}_{t+1} | \mathbf{x}_0)$ all follow known Gaussian distribution, we can derive the analytical form for $q(\mathbf{x}_t | \mathbf{x}_0, \mathbf{x}_{t+1})$. It is easy to verify that it also follows Gaussian distribution and the parameters are derived as Eq. (21). \square

A.5. The Proof of Eq. (31) in Sec. 3.2.2

$$\mathbf{x}_t = \boldsymbol{\eta}_t \mathbf{x}_0, \quad \eta_{t,i} \sim \frac{1}{\alpha_t} \mathcal{G}(\alpha_t, 1), \quad (31)$$

where $t = 0, 1, \dots, N-1$.

Proof. Firstly, we have a known conclusion from probability theory: Suppose $X \sim \mathcal{G}(\alpha, 1)$, $Y \sim \mathcal{G}(\beta, 1)$, then

$$\frac{X}{X+Y} \sim \mathcal{B}(\alpha, \beta),$$

and $X+Y$ is independent to $\frac{X}{X+Y}$.

Based on it, we have a corollary: Suppose U is independent to V and $U \sim \mathcal{B}(\alpha, \beta)$, $V \sim \mathcal{G}(\alpha + \beta, 1)$, then

$$UV \sim \mathcal{G}(\alpha, 1).$$

Now, we prove Eq. (31) according to the definition in Eq. (29) and Eq. (30). It is easy to verify that $\mathbf{x}_1 | \mathbf{x}_0$ is satisfied. Assume $\mathbf{x}_{t-1} | \mathbf{x}_0$ follows $\boldsymbol{\eta}_{t-1} \mathbf{x}_0$, then

$$\mathbf{x}_t | \mathbf{x}_0 \sim \frac{\alpha_{t-1}}{\alpha_t} \boldsymbol{\zeta}_t \boldsymbol{\eta}_{t-1} \mathbf{x}_0,$$

where $\boldsymbol{\eta}_{t-1} \sim \frac{1}{\alpha_{t-1}} \mathcal{G}(\alpha_{t-1}, 1)$, $\boldsymbol{\zeta}_t \sim \mathcal{B}(\alpha_{t+1}, \alpha_t - \alpha_{t+1})$. Since $\boldsymbol{\zeta}_t$ and $\boldsymbol{\eta}_{t-1}$ are independent, $\boldsymbol{\zeta}_t \boldsymbol{\eta}_{t-1} \sim \frac{1}{\alpha_{t-1}} \mathcal{G}(\alpha_t, 1)$. Considering the coefficient, Eq. (31) is proved. \square

A.6. The Proof of Eq. (32) in Sec. 3.2.2

$$\left(\frac{\alpha_t \mathbf{x}_t - \alpha_{t+1} \mathbf{x}_{t+1}}{\mathbf{x}_0} \right)_i \sim \mathcal{G}(\alpha_t - \alpha_{t+1}, 1), t = 1, \dots, N-1. \quad (32)$$

Proof. Similar to Appendix A.4, we still have

$$\begin{aligned} q(\mathbf{x}_t | \mathbf{x}_0, \mathbf{x}_{t+1}) &= \frac{q(\mathbf{x}_t, \mathbf{x}_{t+1} | \mathbf{x}_0)}{q(\mathbf{x}_{t+1} | \mathbf{x}_0)} \\ &= \frac{q(\mathbf{x}_t | \mathbf{x}_0) q(\mathbf{x}_{t+1} | \mathbf{x}_t)}{q(\mathbf{x}_{t+1} | \mathbf{x}_0)}. \end{aligned}$$

Since each component is independent, we prove Eq. (32) by components. We have known the following probability density functions:

$$\begin{aligned} q(x_t | x_0) &= \frac{1}{\Gamma(\alpha_t)} \left(\frac{\alpha_t x_t}{x_0} \right)^{\alpha_t-1} \exp \left\{ -\frac{\alpha_t x_t}{x_0} \right\} \cdot \frac{\alpha_t}{x_0}, \\ q(x_{t+1} | x_0) &= \frac{1}{\Gamma(\alpha_{t+1})} \left(\frac{\alpha_{t+1} x_{t+1}}{x_0} \right)^{\alpha_{t+1}-1} \\ &\quad \cdot \exp \left\{ -\frac{\alpha_{t+1} x_{t+1}}{x_0} \right\} \cdot \frac{\alpha_{t+1}}{x_0}, \\ q(x_{t+1} | x_t) &= \frac{\Gamma(\alpha_t)}{\Gamma(\alpha_{t+1}) \Gamma(\alpha_t - \alpha_{t+1})} \left(\frac{\alpha_{t+1} x_t}{\alpha_t x_t} \right)^{\alpha_{t+1}-1} \\ &\quad \cdot \left(1 - \frac{\alpha_{t+1} x_{t+1}}{\alpha_t x_t} \right)^{\alpha_t - \alpha_{t+1} - 1} \cdot \frac{\alpha_{t+1}}{\alpha_t x_t}. \end{aligned}$$

Applying the equations above, we have that

$$\begin{aligned}
& \frac{q(\mathbf{x}_t | \mathbf{x}_0) q(\mathbf{x}_{t+1} | \mathbf{x}_t)}{q(\mathbf{x}_{t+1} | \mathbf{x}_0)} \\
&= \frac{1}{\Gamma(\alpha_t)} \left(\frac{\alpha_t x_t}{x_0} \right)^{\alpha_t-1} \exp \left\{ -\frac{\alpha_t x_t}{x_0} \right\} \cdot \frac{\alpha_t}{x_0} \\
& \quad \cdot \frac{\Gamma(\alpha_t)}{\Gamma(\alpha_{t+1}) \Gamma(\alpha_t - \alpha_{t+1})} \left(\frac{\alpha_{t+1} x_{t+1}}{\alpha_t x_t} \right)^{\alpha_{t+1}-1} \\
& \quad \cdot \left(1 - \frac{\alpha_{t+1} x_{t+1}}{\alpha_t x_t} \right)^{\alpha_t - \alpha_{t+1} - 1} \cdot \frac{\alpha_{t+1}}{\alpha_t x_t} \\
& \quad / \left(\frac{\left(\frac{\alpha_{t+1} x_{t+1}}{x_0} \right)^{\alpha_{t+1}-1}}{\Gamma(\alpha_{t+1})} \exp \left\{ -\frac{\alpha_{t+1} x_{t+1}}{x_0} \right\} \cdot \frac{\alpha_{t+1}}{x_0} \right) \\
&= \frac{1}{\Gamma(\alpha_t - \alpha_{t+1})} \frac{(\alpha_t x_t)^{\alpha_t-1} (\alpha_{t+1} x_{t+1})^{\alpha_{t+1}-1} x_0^{\alpha_{t+1}-1}}{x_0^{\alpha_t-1} (\alpha_t x_t)^{\alpha_{t+1}-1} (\alpha_{t+1} x_{t+1})^{\alpha_{t+1}-1}} \\
& \quad \cdot \exp \left\{ -\frac{\alpha_t x_t}{x_0} + \frac{\alpha_{t+1} x_{t+1}}{x_0} \right\} \\
& \quad \cdot \left(1 - \frac{\alpha_{t+1} x_{t+1}}{\alpha_t x_t} \right)^{\alpha_t - \alpha_{t+1} - 1} \frac{\alpha_t}{x_0} \cdot \frac{\alpha_{t+1}}{\alpha_t x_t} \cdot \frac{x_0}{\alpha_{t+1}} \\
&= \frac{1}{\Gamma(\alpha_t - \alpha_{t+1})} \frac{(\alpha_t x_t)^{\alpha_t - \alpha_{t+1}}}{x_0^{\alpha_t - \alpha_{t+1}}} \exp \left\{ -\frac{\alpha_t x_t - \alpha_{t+1} x_{t+1}}{x_0} \right\} \\
& \quad \cdot \left(\frac{\alpha_t x_t - \alpha_{t+1} x_{t+1}}{\alpha_t x_t} \right)^{\alpha_t - \alpha_{t+1} - 1} \cdot \frac{1}{x_t} \\
&= \frac{\left(\frac{1}{x_0} \right)^{\alpha_t - \alpha_{t+1}}}{\Gamma(\alpha_t - \alpha_{t+1})} \exp \left\{ -\frac{\alpha_t x_t - \alpha_{t+1} x_{t+1}}{x_0} \right\} \\
& \quad \cdot (\alpha_t x_t - \alpha_{t+1} x_{t+1})^{\alpha_t - \alpha_{t+1} - 1} \cdot \alpha_t.
\end{aligned}$$

Therefore, let $\tau_t = \frac{\alpha_t x_t - \alpha_{t+1} x_{t+1}}{x_0}$, then τ_t follows $\mathcal{G}(\alpha_t - \alpha_{t+1}, 1)$. Thus, Eq. (32) is proved. \square

A.7. The Derivation of Eq. (35) in Sec 3.2.2

$$\begin{aligned}
& D_{\text{KL}}(q(\mathbf{x}_t | \mathbf{x}_0, \mathbf{x}_{t+1}) \| p_\theta(\mathbf{x}_t | \mathbf{x}_{t+1})) \\
&= \sum_i (\alpha_t - \alpha_{t+1}) \left(\log \frac{f_{\theta,i}}{x_{0,i}} + \frac{x_{0,i}}{f_{\theta,i}} - 1 \right). \quad (35)
\end{aligned}$$

Here, f_θ is the abbreviation of $f(\mathbf{x}_{t+1}, t+1; \theta)$.

Proof.

$$\begin{aligned}
& D_{\text{KL}}(q(\mathbf{x}_t | \mathbf{x}_0, \mathbf{x}_{t+1}) \| p_\theta(\mathbf{x}_t | \mathbf{x}_{t+1})) \\
&= \int_q \log \frac{q(\mathbf{x}_t | \mathbf{x}_0, \mathbf{x}_{t+1})}{p_\theta(\mathbf{x}_t | \mathbf{x}_{t+1})} d\mathbf{x}_t \\
&= \sum_i \int_q \left((\alpha_t - \alpha_{t+1}) \log \frac{f_{\theta,i}}{x_{0,i}} - (\alpha_t x_t - \alpha_{t+1} x_{t+1}) \right. \\
& \quad \cdot \left. \left(\frac{1}{x_{0,i}} - \frac{1}{f_{\theta,i}} \right) \right) d\mathbf{x}_t \\
&= \sum_i (\alpha_t - \alpha_{t+1}) \log \frac{f_{\theta,i}}{x_{0,i}} - \mathbb{E}[x_{0,i} \tau_{t,i}] \left(\frac{1}{x_{0,i}} - \frac{1}{f_{\theta,i}} \right) \\
&= \sum_i (\alpha_t - \alpha_{t+1}) \log \frac{f_{\theta,i}}{x_{0,i}} - (\alpha_t - \alpha_{t+1}) x_{0,i} \left(\frac{1}{x_{0,i}} - \frac{1}{f_{\theta,i}} \right) \\
&= \sum_i (\alpha_t - \alpha_{t+1}) \left(\log \frac{f_{\theta,i}}{x_{0,i}} + \frac{x_{0,i}}{f_{\theta,i}} - 1 \right).
\end{aligned}$$

\square

A.8. The Proof of Eq. (36) in Sec 3.2.2

Suppose f_{θ^*} is the optimal function minimizing Eq. (35), it is also the optimal function for the following optimization problem:

$$\min_{f_\theta} \mathbb{E}_q \|f(\mathbf{x}_{t+1}, t+1; \theta) - \mathbf{x}_0\|_2^2. \quad (36)$$

Proof. Minimizing KL divergence is equivalent to

$$\mathbb{E}_q \sum_i \left[(\alpha_{i-1} - \alpha_i) \left(\log \frac{f(\mathbf{x}_{t+1}, t; \theta)_i}{x_0} + \frac{x_{0,i}}{f(\mathbf{x}_{t+1}, t; \theta)_i} \right) \right].$$

Given t and \mathbf{x}_t , according to [22] the optimal $f(\mathbf{x}_{t+1}, t; \theta)$ satisfies that

$$\arg \min_{\beta} \int q(\mathbf{x}_0 | \mathbf{x}_{t+1}) \sum_i \left(\log \frac{\beta_i}{x_{0,i}} + \frac{x_{0,i}}{\beta_i} \right) d\mathbf{x}_0.$$

We compute the gradient of β for the right part and derive that

$$\int q(\mathbf{x}_0 | \mathbf{x}_{t+1}) \left(\frac{1}{\beta} - \frac{x_0}{\beta^2} \right) d\mathbf{x}_0.$$

Let the gradient to be $\mathbf{0}$ (we can neglect the situation where $\beta = 0$), we have

$$\int q(\mathbf{x}_0 | \mathbf{x}_{t+1}) (\beta - \mathbf{x}_0) d\mathbf{x}_0 = \mathbf{0}.$$

When $\beta = \mathbb{E}[\mathbf{x}_0 | \mathbf{x}_{t+1}]$, it is the optimal solution. Therefore, the optimal $f(\mathbf{x}_{t+1}, t; \theta)$ should be $\mathbb{E}[\mathbf{x}_0 | \mathbf{x}_{t+1}]$. That is to say, training $f(\mathbf{x}_{t+1}, t; \theta)$ by minimizing KL divergence is equivalent to minimize

$$\mathbb{E}_q \|f(\mathbf{x}_{t+1}, t; \theta) - \mathbf{x}_0\|_2^2.$$

\square

A.9. The Proof of Eq. (41) in Sec 3.2.3

$$\mathbf{x}_t \mid \mathbf{x}_0 \sim \frac{\mathcal{P}(\lambda_t \mathbf{x}_0)}{\lambda_t}, \quad (41)$$

where $t = 1, \dots, N-1$.

Proof. Firstly, Eq. (41) holds when $t = N$. Assume that $\mathbf{x}_{t+1} \mid \mathbf{x}_0$ holds, then

$$\begin{aligned} \mathbf{x}_t \mid \mathbf{x}_0 &\sim \frac{\lambda_{t+1} \mathbf{x}_{t+1} \mid \mathbf{x}_0 + \mathcal{P}((\lambda_t - \lambda_{t+1}) \mathbf{x}_0)}{\lambda_t} \\ &\sim \frac{\mathcal{P}((\lambda_{t+1}) \mathbf{x}_0) + \mathcal{P}((\lambda_t - \lambda_{t+1}) \mathbf{x}_0)}{\lambda_t} \\ &\sim \frac{\mathcal{P}(\lambda_t \mathbf{x}_0)}{\lambda_t}. \end{aligned}$$

□

A.10. The Derivation of Eq. (46) in Sec 3.2.3

$$\begin{aligned} D_{\text{KL}}(q(\mathbf{x}_t \mid \mathbf{x}_0, \mathbf{x}_{t+1}) \parallel p_\theta(\mathbf{x}_t \mid \mathbf{x}_{t+1})) \\ = \sum_i (\log x_{0,i} - \log f_{\theta,i}) (\lambda_t - \lambda_{t+1}) x_{0,i} \\ - (\lambda_t - \lambda_{t+1}) (x_{0,i} - f_{\theta,i}), \end{aligned} \quad (46)$$

where $f(\mathbf{x}_{t+1}, \mathbf{x}_N, t+1; \theta)$ is denoted as f_θ for simplicity.

Proof. Let $\tau_t = \lambda_t \mathbf{x}_t - \lambda_{t+1} \mathbf{x}_{t+1}$. For simplicity, we regard all vectors as variables. Then, we have the following derivation

$$\begin{aligned} D_{\text{KL}}(q(\mathbf{x}_t \mid \mathbf{x}_0, \mathbf{x}_{t+1}) \parallel p_\theta(\mathbf{x}_t \mid \mathbf{x}_{t+1})) \\ = \sum_{\mathbf{x}_t} q(\mathbf{x}_t \mid \mathbf{x}_0, \mathbf{x}_{t+1}) \log \frac{q(\mathbf{x}_t \mid \mathbf{x}_0, \mathbf{x}_{t+1})}{p_\theta(\mathbf{x}_t \mid \mathbf{x}_{t+1})} \\ = \sum_{\tau_t} \frac{(\lambda_t - \lambda_{t+1})^{\tau_t} x_0^{\tau_t}}{\tau_t!} e^{-(\lambda_t - \lambda_{t+1}) x_0} \\ \cdot \log \frac{(\lambda_t - \lambda_{t+1})^{\tau_t} x_0^{\tau_t} e^{-(\lambda_t - \lambda_{t+1}) x_0}}{(\lambda_t - \lambda_{t+1})^{\tau_t} f_\theta^{\tau_t} e^{-(\lambda_t - \lambda_{t+1}) f_\theta}} \\ = \sum_{\tau_t} \frac{(\lambda_t - \lambda_{t+1})^{\tau_t} x_0^{\tau_t}}{\tau_t!} e^{-(\lambda_t - \lambda_{t+1}) x_0} \\ \cdot ((\log x_0 - \log f_\theta) \tau_t - (\lambda_t - \lambda_{t+1}) (x_0 - f_\theta)) \\ = (\log x_0 - \log f_\theta) \mathbb{E}[\tau_t] - (\lambda_t - \lambda_{t+1}) (x_0 - f_\theta) \\ = (\log x_0 - \log f_\theta) (\lambda_t - \lambda_{t+1}) x_0 - (\lambda_t - \lambda_{t+1}) (x_0 - f_\theta). \end{aligned}$$

Therefore, Eq. (46) is proved.

□

A.11. The Proof of Eq. (47) in Sec 3.2.3

Suppose f_{θ^*} is the optimal function minimizing Eq. (46), it is also the optimal function for the following optimization problem:

$$\min_{f_\theta} \mathbb{E}_q \|f(\mathbf{x}_{t+1}, \mathbf{x}_N, t+1; \theta) - \mathbf{x}_0\|_2^2. \quad (47)$$

Proof. Minimizing KL divergence is equivalent to

$$\begin{aligned} \mathbb{E}_{\mathbf{x}_0, \mathbf{x}_{t+1}} \sum_i (\log x_{0,i} - \log f_{\theta,i}) (\lambda_t - \lambda_{t+1}) x_{0,i} \\ - (\lambda_t - \lambda_{t+1}) (x_{0,i} - f_{\theta,i}). \end{aligned}$$

Given t and \mathbf{x}_t , according to [22] the optimal $f(\mathbf{x}_{t+1}, \mathbf{x}_N, t; \theta)$ satisfies that

$$\begin{aligned} \arg \min_s \int q(\mathbf{x}_0 \mid \mathbf{x}_{t+1}, \mathbf{x}_N) \sum_i ((\log x_{0,i} - \log s_i) \\ \cdot (\lambda_t - \lambda_{t+1}) x_{0,i} - (\lambda_t - \lambda_{t+1}) (x_{0,i} - s_i)) d\mathbf{x}_0. \end{aligned}$$

We compute the gradient of s for the right part and derive that

$$\int q(\mathbf{x}_0 \mid \mathbf{x}_{t+1}, \mathbf{x}_N) \left(-(\lambda_t - \lambda_{t+1}) \frac{\mathbf{x}_0}{s} + (\lambda_t - \lambda_{t+1}) \right) d\mathbf{x}_0.$$

Let the gradient to be $\mathbf{0}$, we have

$$\begin{aligned} \int q(\mathbf{x}_0 \mid \mathbf{x}_{t+1}, \mathbf{x}_N) \left(-\frac{\mathbf{x}_0}{s} + 1 \right) d\mathbf{x}_0 \\ = -\frac{\mathbb{E}[\mathbf{x}_0 \mid \mathbf{x}_{t+1}, \mathbf{x}_N]}{s} + 1 = \mathbf{0}. \end{aligned}$$

When $s = \mathbb{E}[\mathbf{x}_0 \mid \mathbf{x}_{t+1}, \mathbf{x}_N]$, it is the optimal solution. Therefore, the optimal $f(\mathbf{x}_{t+1}, \mathbf{x}_N, t; \theta)$ should be $\mathbb{E}[\mathbf{x}_0 \mid \mathbf{x}_{t+1}, \mathbf{x}_N]$. That is to say, training $f(\mathbf{x}_{t+1}, \mathbf{x}_N, t; \theta)$ by minimizing KL divergence is equivalent to minimize

$$\mathbb{E}_q \|f(\mathbf{x}_{t+1}, \mathbf{x}_N, t; \theta) - \mathbf{x}_0\|_2^2.$$

□

B. Experimental Details

Parameters Sequence For simplicity, suppose $\{\alpha_t\}$ is the parameters sequence used for constructing the diffusion process. Let σ_{α_t} represent the standard deviation of $\mathbf{x}_t \mid \mathbf{x}_0$ from $t = 0$ to $t = N$ where N is the diffusion steps. We have that $\sigma_{\alpha_0} = 0$ and σ_{α_N} is known. We set

$$\sigma_{\alpha_t} = \frac{t}{N} * \sigma_{\alpha_N}$$

and ascertain the value of α_t according to σ_{α_t} .

The Effect of Steps N For Gaussian noise with $\sigma = 25$, Gamma noise with $\alpha = 26$ and Poisson noise with $\lambda = 0.2$, we also conduct experiments where $N = 10$ and compare the result to $N = 20$. The result is shown in Tab. 2 and Fig. 4. From the metrics and visual quality, our method also achieve satisfied performance even with $N = 10$.

Noise Model	Kodak			CSet9		
	SL	Samples	Mean of Samples	SL	Samples	Mean of Samples
Gaussian, $\sigma = 25$	30.53 / 0.816	28.62 / 0.761	30.48 / 0.821	29.41 / 0.843	27.61 / 0.800	29.44 / 0.849
Gamma, $\alpha = 26$	31.18 / 0.849	29.35 / 0.796	31.16 / 0.851	29.68 / 0.854	27.98 / 0.807	29.76 / 0.856
Poisson, $\lambda = 0.2$	30.95 / 0.834	28.88 / 0.776	30.46 / 0.835	29.68 / 0.851	27.69 / 0.800	29.25 / 0.853

Table 2. Quantitative comparison in terms of PNSR (dB) / SSIM for different noise model on Kodak and CSet9 datasets. The number of diffusion steps is set as 10. We compare supervised learning (SL) to our method. "Samples" means the generated results while "Mean of Samples" means the average of 100 samples for each noisy images.

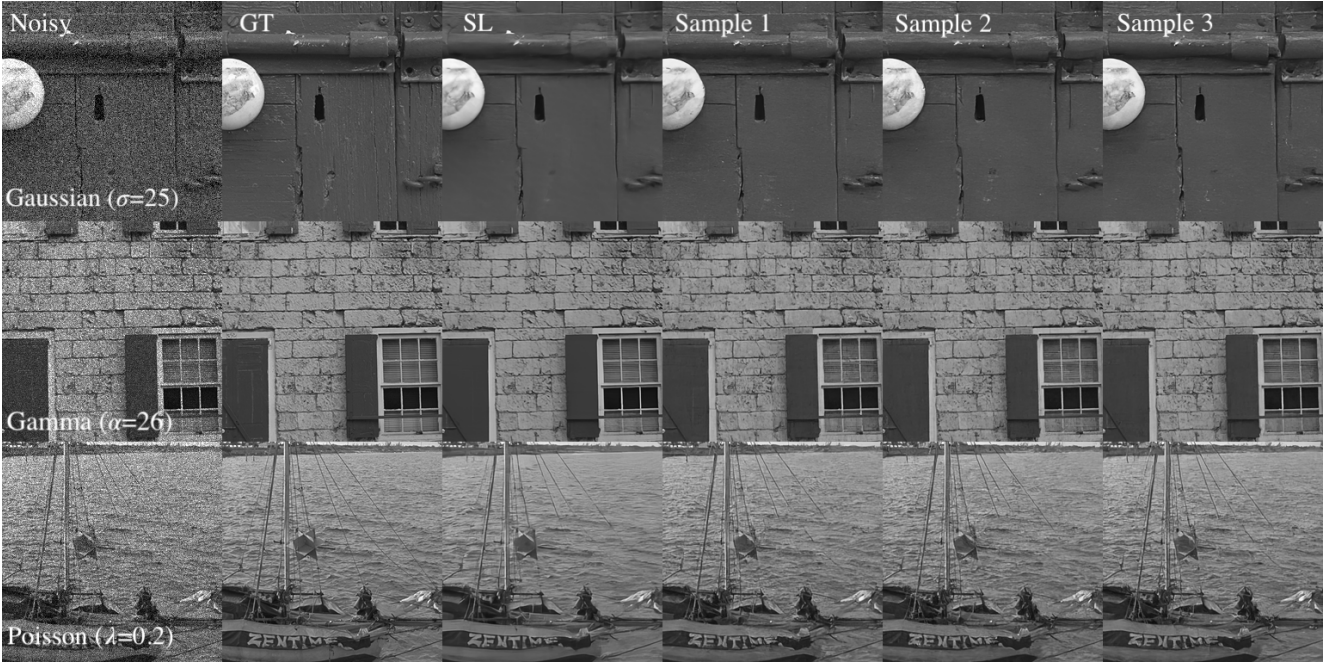


Figure 4. Qualitative comparison using Kodak dataset. From top to bottom is: Gaussian noise with $\sigma = 25$, Gamma noise with $\alpha = 26$, and Poisson noise with $\lambda = 0.2$. Noisy: noisy image, GT: ground-truth, SL: supervised learning. The last three columns are generated different samples using $N = 10$.